ALEPH 95-032
PHYSIC 95-030
9 March 1995

Measurement of the $B_d^0 - \overline{B_d^0}$ Oscillation Frequency using a Jet-Charge Method

S. Emery and W. Kozanecki

March 9, 1995

Abstract

$B_d^0 - \overline{B_d^0}$ oscillation is studied using hadronic Z decays collected by the ALEPH experiment at LEP. The sample is enriched in primary b semileptonic decays by selecting events that contain at least one high transverse momentum lepton and two jets. A topological vertexing technique is applied to measure the decay length of the b hadrons, and their momentum is determined using an energy flow technique. The charge of the decaying b quark is tagged by the electron or muon, and its charge at production time is extracted from the momentum-weighted average of the charges of jet fragments in the hemisphere opposite to the lepton. Based on the analysis of approximately 1.7 million Z decays recorded in 1991-1993, we measure $\Delta m_d = 0.433^{+0.050}_{-0.032}(\text{stat.})^{+0.062}_{-0.064}(\text{syst.})\ \text{ps}^{-1}$.

1 Introduction

The measurement of Δm_d in inclusive semileptonic b-decays at LEP was first reported by ALEPH, using the dilepton method [1]. In that approach, the charge of a b quark is tagged at both production and decay time by leptons, originating from primary b decays in the event hemisphere respectively opposite to, and the same as, the hemisphere containing the B^0 .

The advantages of the dilepton method are a very high b-purity, and, more importantly, a relatively low mistag rate: the lepton charge is diluted almost exclusively by the $b \to c \to l$ cascade decays. The counterpart is that the statistical power of the method is limited by an event rate proportional to the square of the b semileptonic branching ratio.

In this report, we extend the method developed in [1, 2] to the case of inclusive lepton-jet events, containing (at least) one high transverse momentum lepton, and at least two jets. The flight time of the b hadron that produced the lepton is measured by essentially the same method as in the dilepton analysis. Its nature (particle or antiparticle) at decay time is also inferred from the decay lepton; but the charge of the b quark at production time is inferred from the jet charge in the opposite hemisphere. As only one semileptonic decay is required, the size of the event sample increases by approximately a factor of ten; the statistical gain is however partially diluted by the higher mistag rate associated with jet-charge tagging. The technique presented here is similar to the recently released study of B_s^0 oscillations [3]. But the problems, and systematics, of measuring Δm_d are different from those associated with putting a limit on Δm_s , so the two analyses differ in a number of aspects.

This report is organized as follows. The jet charge concepts used in this analysis, and the methodology of the measurement, are defined in Sec. 2. Sec. 3 describes the event selection and the flavor composition of the lepton-jet sample. The measurement of the flight distance, the b hadron momentum reconstruction, and the treatment of time resolution functions are discussed in Sec. 4. The measurement of Δm_d , based on a fit to the time dependence of the average lepton-signed jet charge, forms the subject of Sec. 5. Systematic errors are studied in Sec. 6. Our findings are summarized in Sec. 7.

2 Methodology

The principle of the method is illustrated in Fig. 1. A b hadron decays to a lepton after having possibly undergone an oscillation; the charge of the decaying quark, and the decay time itself, are related, respectively, to the lepton charge, and to the distance between the primary event vertex and the lepton decay vertex. The charge of that same b quark at production time is extracted from the jet charge in the hemisphere opposite to the lepton.

We define the hemisphere charge (or "jet" charge, for short) as

$$Q_H = \frac{\sum_i |\vec{p}_i \cdot \vec{e}_T|^\kappa \cdot q_i}{\sum_i |\vec{p}_i \cdot \vec{e}_T|^\kappa} \tag{1}$$

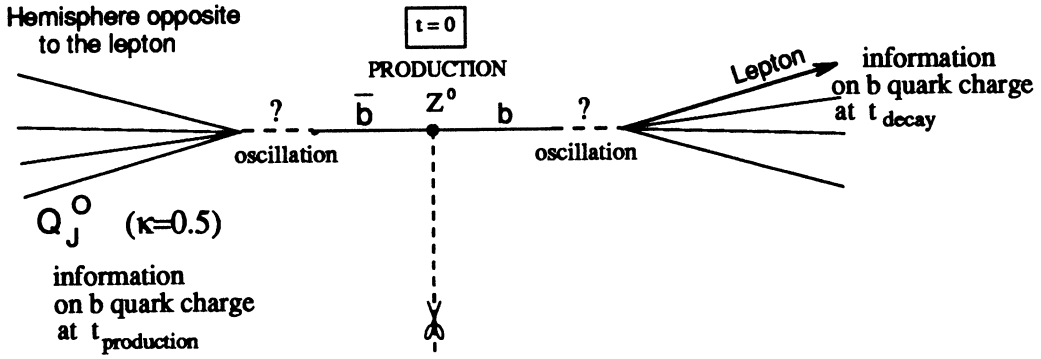

Figure 1: Principle of Δm_d measurement using lepton-jet events.

as the momentum-weighted charge average over all charged particles in that hemisphere. $|\vec{p}_i \cdot \vec{e}_T|$ is the momentum component of particle i along the thrust axis, q_i is its charge, and the momentum-weighting exponent $\kappa = 0.5$ is chosen to maximize the charge separation power for average b jets [4]. We further define the lepton-signed hemisphere charge

$$Q_{lH} = \langle -q_l \times Q_H \rangle \tag{2}$$

as the average, over the sample of lepton-jet pairs, of the product of the lepton charge by the jet charge in the hemisphere opposite to the lepton.

For a pure sample of $b \to l$ decays, and to the extent that the hemisphere charge Q_H properly reflects, on the average, the charge sign of the parent quark in its hemisphere, the quantity Q_{lH} is positive for that event sample in which the lepton originates from a B meson that did not mix, and negative if that lepton was produced by a B^0 that had oscillated to its antiparticle. The basic quantity we measure is therefore $Q_{lH}(t)$, the time-dependence of the lepton-signed jet charge. It is simply related to the oscillation frequencies:

$$\begin{aligned} Q_{lH}(t) &= < Q_H \times sign(q^{opp}_{quark}) > \times < q_l \times sign(q^{lep}_{quark}) > (t) \\ &= - \underbrace{Q_b}_{amplitude} \times (1 - f_d - f_s + f_d \cos(\underbrace{\Delta m_d}_{frequency} t) + f_s \cos(\Delta m_s t)) \end{aligned} \tag{3}$$

In this equation, q^{opp}_{quark} is the charge of the primary quark in the hemisphere opposite to the lepton, and q^{lep}_{quark} that of the primary quark in the lepton hemisphere. The first term, Q_b, is the average charge of a b jet. The second term is the average lepton charge, and exhibits a time-independent contribution from charged B mesons and B baryons, and oscillation terms, corresponding to B_d's and B_s's, and proportional to f_d and f_s, the fractions of leptons originating from primary $b \to l$ decays of B^0_d and B^0_s mesons, respectively. This simplified formula must be generalized to take into account $b \to c \to l$ decays, as well as backgrounds from charm, nonprompt leptons and misidentified hadrons; this will be treated in Sec. 5.

It is a matter of simple algebra to show that the lepton-signed hemisphere charge is a straightforward generalization of the same-sign fraction $Q(t)$ used in the dilepton analysis (Eq. (7) in Ref. [1]). Replacing the hemisphere charge by that of the second

lepton, the relationship is

$$Q_{lH} \rightarrow Q_{ll} = 1 - 2Q(t) \tag{4}$$

In the dilepton case, there is no conceptual distinction between same-sign fraction and average lepton-signed charge because lepton charges are discrete (± 1). In the jet charge case, however, two approaches are possible. Analyses such as that of Ref. [3] also define a same-sign fraction, by comparing the sign of the lepton to that of the jet charge; no use is made of the numerical value of the jet charge, except for rejecting those events where it is close to 0. In contrast, we prefer to keep all events irrespective of the numerical value of the jet charge, and to express our measurement in terms of the average, untruncated value of Q_{lH}. It has been shown [5] that this procedure has at least as good a statistical power as the same-sign-fraction method with optimized truncation.

An additional difference between our analysis and that of Ref. [3] is the choice of the momentum weighting scheme. While Ref. [3] combines the jet charges in the lepton hemisphere and the one opposite, we restrict ourselves to the opposite-hemisphere charge, because of the sensitivity of the Δm_d measurement to a proper treatment of the $b \rightarrow c \rightarrow l$ channel. The simple relationship $Q_{lH}(b \rightarrow l^-) = -Q_{lH}(b \rightarrow c \rightarrow l^+)$, that reflects the flip in the lepton sign, is only valid as long as the lepton in no way intervenes in the jet charge Q_H itself. Combining the jet charge in the two hemispheres forces one to rely on the Monte Carlo for at least some of the average jet charges (or mistag fractions, in the language of Ref. [3]). This is true not only for the cascades, but actually for all average B jet charges ($B^{\pm}$ and B hadrons, B_d and B_s, mixed and unmixed, primary and cascade decays). We prefer to avoid such a model dependence, by treating the average b jet charge as a free parameter in the fit to $Q_{lH}(t)$. Having thus opted for the use of the opposite-hemisphere charge only, it has been shown [4] that the optimum weighting scheme, for the average b jet, is momentum weighting with the exponent κ as chosen here.

3 Event Selection and Sample Composition

The topology used in this analysis is that of hadronic Z events containing at least one lepton that originates from a primary $b \rightarrow l$ decay. The hemisphere opposite the lepton is treated in an inclusive fashion; in particular, if an event contains several leptons passing all the cuts, all "lepton-opposite hemisphere" pairs (hereafter called "lepton-jet" pairs for the sake of brevity) are considered independently in the analysis.

Specifically, the selection criteria are the following:

- Data are selected from the 1991 to 1993 Mini-DST runs that satisfy PERFECT or MAYBE, and the electroweak and heavy flavor quality criteria.
- The event must pass the hadronic event selection (Class 16).
- It must contain at least two jets, reconstructed with the Jade algorithm applied to qualifying energy flow objects (excluding Sical), with $y_{cut} = (6\ GeV/E_{LEP})^2$.

- The thrust axis, reconstructed from all qualifying energy flow objects, must satisfy $|cos\ \theta_{thrust}| < .85$.
- The event must contain at least one electron or muon, identified on the basis of the standard ALEPH lepton identification criteria [6], and satisfying $p > 3\ GeV/c$, $p_\perp > 1.25\ GeV/c$. The lepton transverse momentum with respect to the nearest jet, $p_\perp$, is defined with the lepton excluded from the jet. To qualify, this lepton must have at least one VDET hit in each of the z and $R\phi$ projections, and the VDET must be in good working order (XDVEOK).

The total number of lepton-jet pairs passing the above criteria (and containing a valid secondary vertex as defined in Sec. 4), is 36507 (14438 electrons, 22069 muons). The sample composition was determined by the method reported in Ref. [7], but with the uds background inflated [8] [1]. The flavor composition of the sample is summarized in Table 1.

Table 1: Flavor composition of the lepton sample after all event, lepton and vertex selection cuts.

Lepton source	Electrons	Muons	All
$b \rightarrow lepton$	0.835	0.732	0.772
$b \rightarrow c \rightarrow lepton$	0.067	0.066	0.067
$c \rightarrow lepton$	0.055	0.058	0.057
$Non - prompt + misid$	0.043	0.144	0.104

4 Proper Time Reconstruction

The proper time is reconstructed as the product of the flight distance d, by the boost factor $g = m_B/p_B c$. The procedure mostly follows that of the dilepton analysis [1], so only the main points will be recalled here. The flight distance and momentum reconstruction are optimized for the $b \rightarrow l$ topology; their performance will be different for $b \rightarrow c \rightarrow l$, $c \rightarrow l$ and background leptons. This will be taken into account, in the modelling of the measured time distribution, by efficiency and resolution functions different for each lepton source.

4.1 Flight Distance Reconstruction

After subdividing the event in two hemispheres perpendicular to the thrust axis, the primary vertex is reconstructed using QFNDIP. A search for a secondary (charm-

[1] Technically, we have used the p, $p_\perp$-dependent fractions supplied by the CALPOIDS package for the 1991 lepton efficiency maps, as those factors are unavailable for subsequent data years. In addition, the contribution of non-prompt leptons and misidentified hadrons from *uds* events has been inflated by a factor of 1.4, corresponding to approximately half of the correction recommended in Ref. [8]. The uncertainties inherent to this procedure have been included in the systematic error (Sec. 6); in particular, the error on the lepton background from *all* sources (not only *uds*) was taken equal in size (±40%) to the *uds* correction.

like) vertex is then performed in the lepton hemisphere, using QVSRCH applied to all tracks except the lepton itself. Tracks passing standard QVSRCH quality cuts are assigned to the secondary vertex if they satisfy [2] $p > 1.5\ GeV/c$ and $\chi^2_{charm} < 2$, where χ^2_{charm} refers to the quality of the track association to the charm vertex found by QVSRCH. The tracks defined as secondary by this procedure are then fitted to a common vertex; the sum of their momenta is used to define the direction of the "charm" track, constructed so it passes through the decay vertex. If only one such track is found, it is taken as the charm candidate; if no charm track is found, the lepton is rejected. The charm track is finally vertexed with the lepton, to give the b decay point. A cut of $\chi^2 < 25$ is applied to the b decay vertex. The b flight distance is taken as the distance in space between the primary and b decay vertices, projected onto the jet axis.

The distance resolution for $b \rightarrow l$ decays, as determined from the Monte Carlo, is shown in Fig. 2, for various slices of true distance. That the resolution depends on the distance itself is clearly apparent; this is due at least in part to primary tracks being misassigned to the secondary vertex and "pulling" the latter back to the primary. The resolution is also different for cascade leptons, as expected from the difference in event topology.

Not only does the resolution vary with distance, but so does the vertexing efficiency. This is shown in Fig. 3, which displays, as a function of true proper time, the fraction of $b \rightarrow l$ leptons that pass all the vertexing cuts, normalized to the number of $b \rightarrow l$ leptons after all cuts *except* vertexing. This function (also different between primary leptons and cascades) will be used, in parametrized form, when convoluting the parent time distribution of b hadrons with the resolution function.

4.2 b hadron Momentum Measurement

The hadron momentum is estimated by the sum of:

- the lepton energy and the sum of the charged energies at the c decay vertex, which together represent about 65 % of the true b energy;
- the missing energy in the hemisphere, typically 21 % of the b energy;
- the neutral electromagnetic energy in the jet of the lepton (10 %);
- finally, a small correction (4 % on the average), proportional to the observed neutral electromagnetic energy, as determined from the simulation. It accounts for the contributions of neutral hadronic energy (not used directly because it is poorly reproduced in the Monte Carlo), and for electromagnetic neutral energy incorrectly assigned to the b hadron by the jet clustering algorithm.

The resolution function for the boost factor g is shown in Fig. 4. The b momentum is clearly underestimated for cascades, because the balance between the

[2] These cuts are stricter than the one used in the dilepton analysis ($\chi^2_{charm} < 9$), as we found they efficiently reduce the fraction of primary tracks unduly associated to the charm vertex.

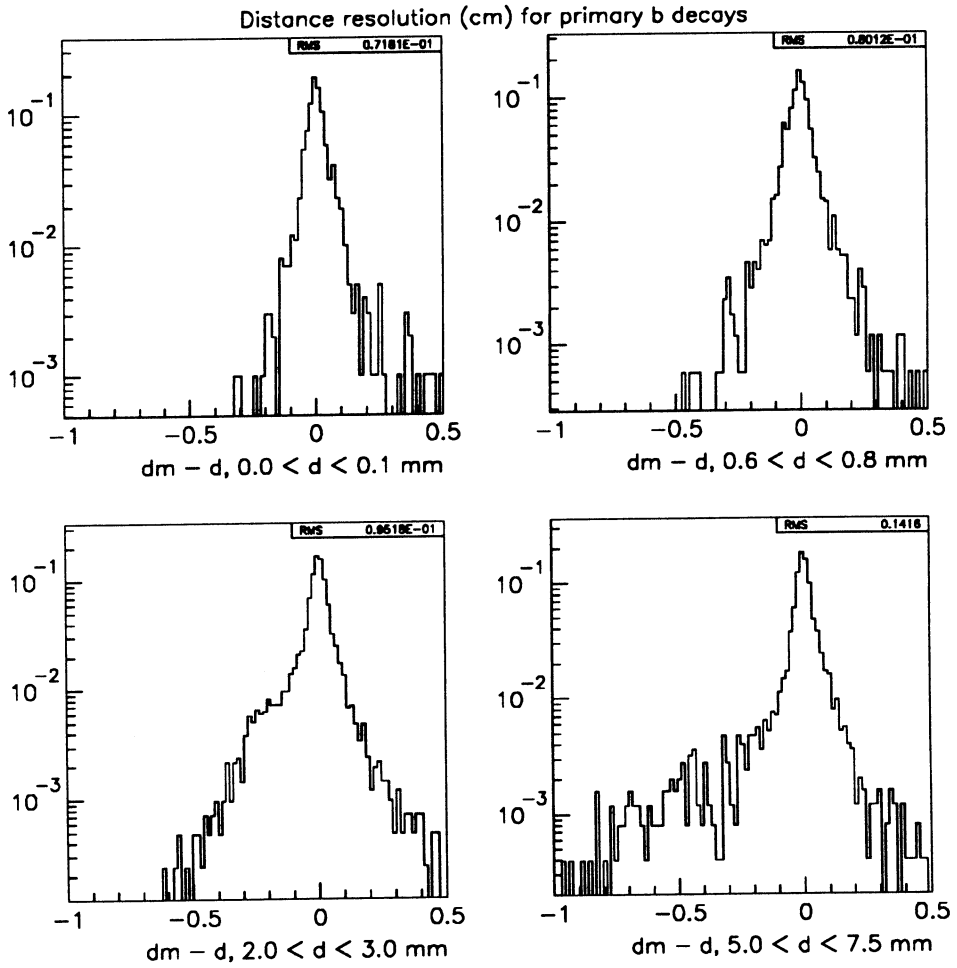

Figure 2: Distance resolution for primary b leptons, for various slices of true distance. The "bump" developing at negative distance is due to track misassignments. The logarithmic scale was chosen to exemplify the shape evolution; a quantitative perception of the importance of misassignments may be better obtained from Fig. 5.

charged, neutral and missing energy components is different from that in $b \rightarrow l$ decays, for which the method was optimized. This is taken into account in the time resolution function.

4.3 Modelling the Proper Time Distribution

The measured proper time distribution of the lepton-jet sample selected in Sec. 3 is the superposition of the distributions corresponding to the flavor subprocesses of Table 1. We detail in this section how each one of those components is modelled, and how they are then combined in view of fitting the average b lifetime to the time distribution measured in data.

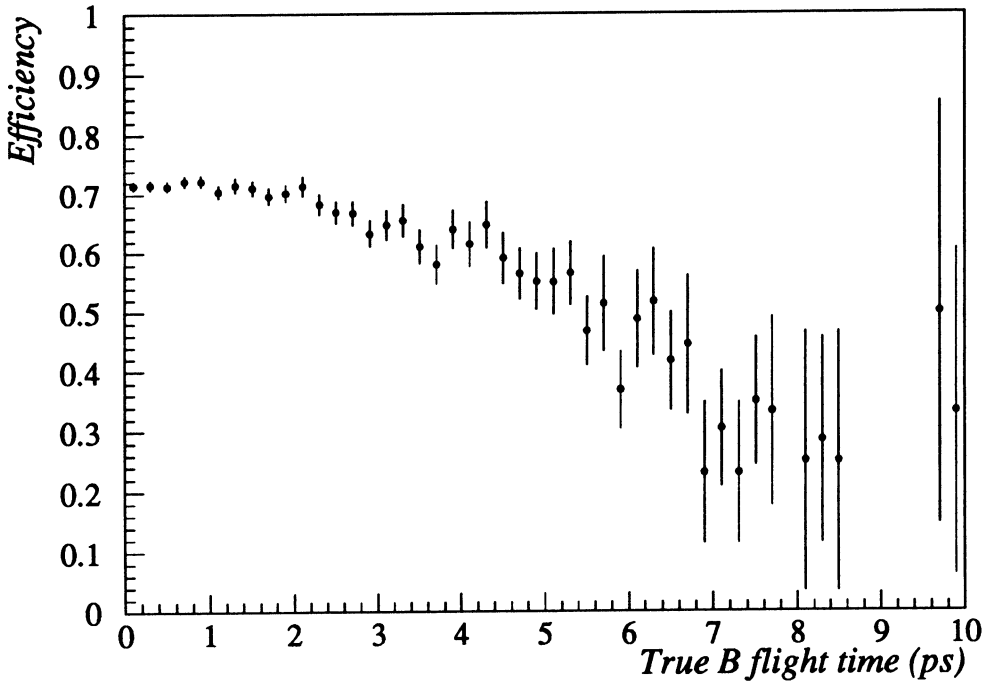

Figure 3: Vertexing efficiency for $b \rightarrow l$ leptons, as a function of true proper time.

4.3.1 Resolution functions

Track misassignments induce a distance dependence in both the distance and the energy resolution function; these two are therefore correlated. This is why, rather than convoluting the g and d resolution functions, we choose to express the resolution function directly in terms of proper time. To this effect, the Monte Carlo was used to produce a parametrization (Fig. 5) of the distributions of $t_m - t$, where t_m is the measured time, in slices of true proper time t. A total of 16 slices were used for $b \rightarrow l$ leptons. The width of the slices was chosen to properly reproduce, after all convolutions, the measured proper time distribution in the Monte-Carlo, while at the same time preventing the parametrization from "following" statistical fluctuations in the MC. A similar procedure was followed for $b \rightarrow c \rightarrow l$ leptons, with 7 slices; examples are shown in Fig. 6.

The resolution in distance can be at least partially checked on data, by selecting fake leptons, i.e. charged tracks that satisfy the same geometrical and kinematical cuts as the leptons, but are required to fail the electron and muon identification criteria. As was observed in other analyses [1, 3], the comparison, between data and Monte Carlo, of the flight distance distributions for fake leptons in *uds*-enriched events, suggests the resolution is slightly optimistic in the Monte Carlo. A fit to the negative tail of the distance distribution for fake leptons, suggests a widening of the resolution by 7.2 $\pm$ 1.4%. This correction was applied, as a global scale factor, to

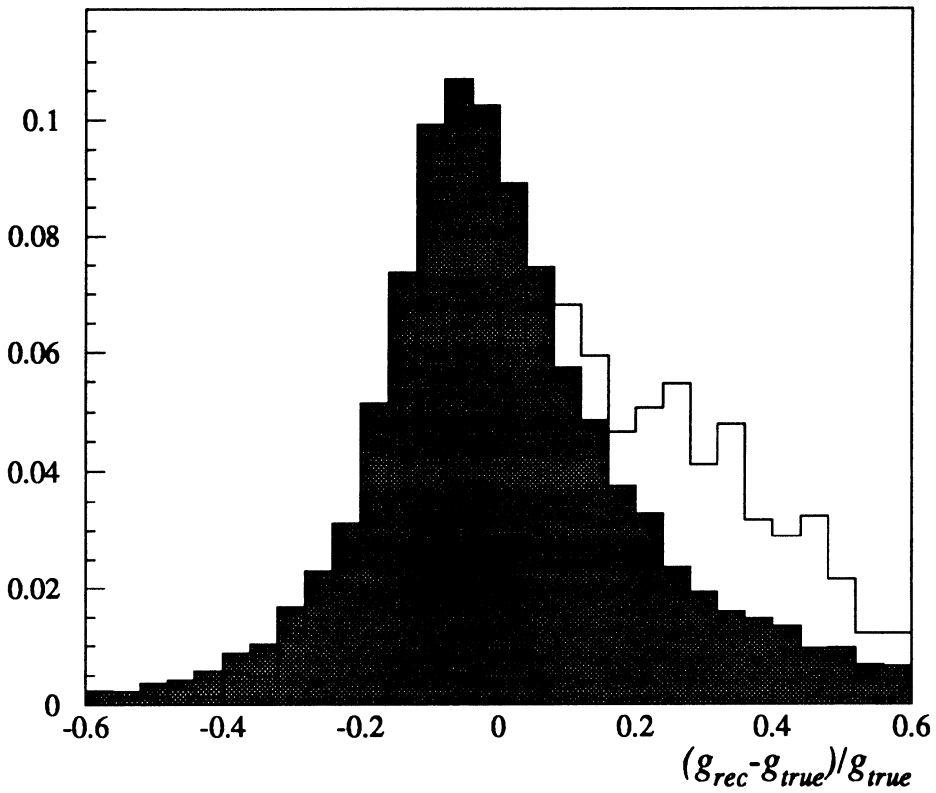

Figure 4: Boost resolution for primary b leptons (shaded), and cascades (unshaded). The RMS widths are, respectively, 20 % and 22 %.

the width of our time resolution function, in all slices of proper time, when analyzing real data. While this procedure properly accounts for distortions of the resolution function at short flight distances, it is not necessarily strictly correct at all distances, because of the distance-dependence of the resolution. This will be fully covered by the systematic error.

4.3.2 Predicted proper time distributions for flavor subprocesses

Starting from a "true" proper time distribution, with a given lifetime (typically 1.5 ps), the measured time distribution for $b \rightarrow l$ decays is obtained by first weighing the parent t distribution by the distance-dependent efficiency function mentioned in Sec. 4.1. The resulting distribution is then convoluted with the time-dependent resolution function of Sec. 4.3.1. A similar procedure is followed for cascade leptons, starting from the same parent time distribution as for $b \rightarrow l$ decays, but with the appropriate efficiency and resolution functions. For charm and backgrounds, the predicted t_m distribution is taken directly from the Monte-Carlo.

These four underlying distributions can then be combined, in the proportions

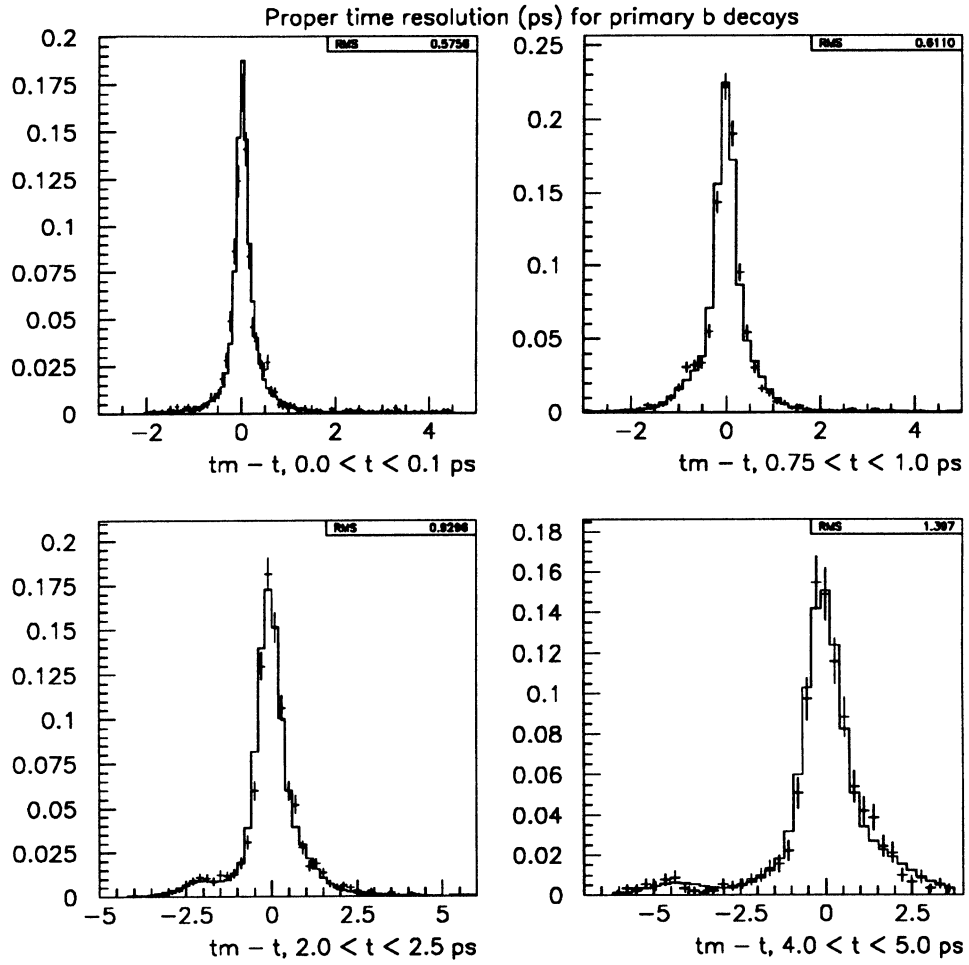

Figure 5: Time resolution for primary b leptons, in slices of true proper time. The points with error bars are the fully simulated data, and the curve is the parametrization of the resolution function.

listed in Table 1, and fitted to the proper time distribution measured in the data by varying the average b lifetime in the parent t distribution.

4.3.3 Fit of the average b lifetime

A correct measurement of the average b lifetime is an important consistency check on our resolution-unfolding procedure.

Fig. 7 displays the measured time distribution in the ALEPH Monte-Carlo. For an input value $\tau_b = 1.5$ ps, the fit returns 1.508 ± 0.015 ps, with $\chi^2/DOF = 59/49$. The residual plot shows no distortions.

Repeating the procedure for the data, one measures $\tau_b = 1.525 \pm 0.013$ (stat.) ps, consistent with the world average. But the fit is poor (Fig. 8): $\chi^2/DOF = 88/49$,

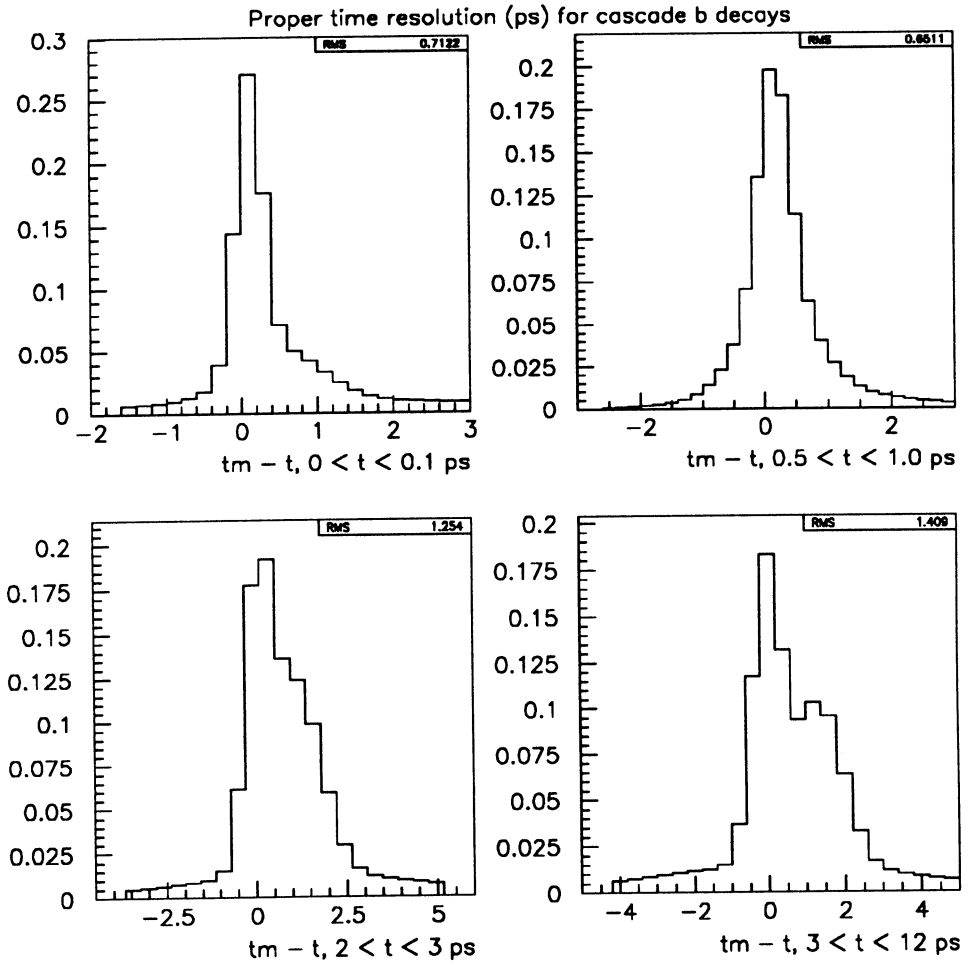

Figure 6: Time resolution for cascade leptons, in various slices of true proper time.

with the dominant distortion arising between -.5 and 2.0 ps. A detailed study of the possible source of this discrepancy suggests it is due to differences, between data and Monte Carlo, in the rate of track misassignments from the primary to the charm vertex; but the problem remains to be fully understood. The same effect was observed in the B_s^0 oscillation analysis of Ref. [3], where it was taken into account by adding a zero-lifetime component to the true parent time distribution of b hadrons, in such a way as to reproduce the measured time distribution. Rather than resorting to the same artifact, we will show in Sec. 5 that our result is stable with respect to a cut on the minimum measured time, that eliminates the region of poor agreement.

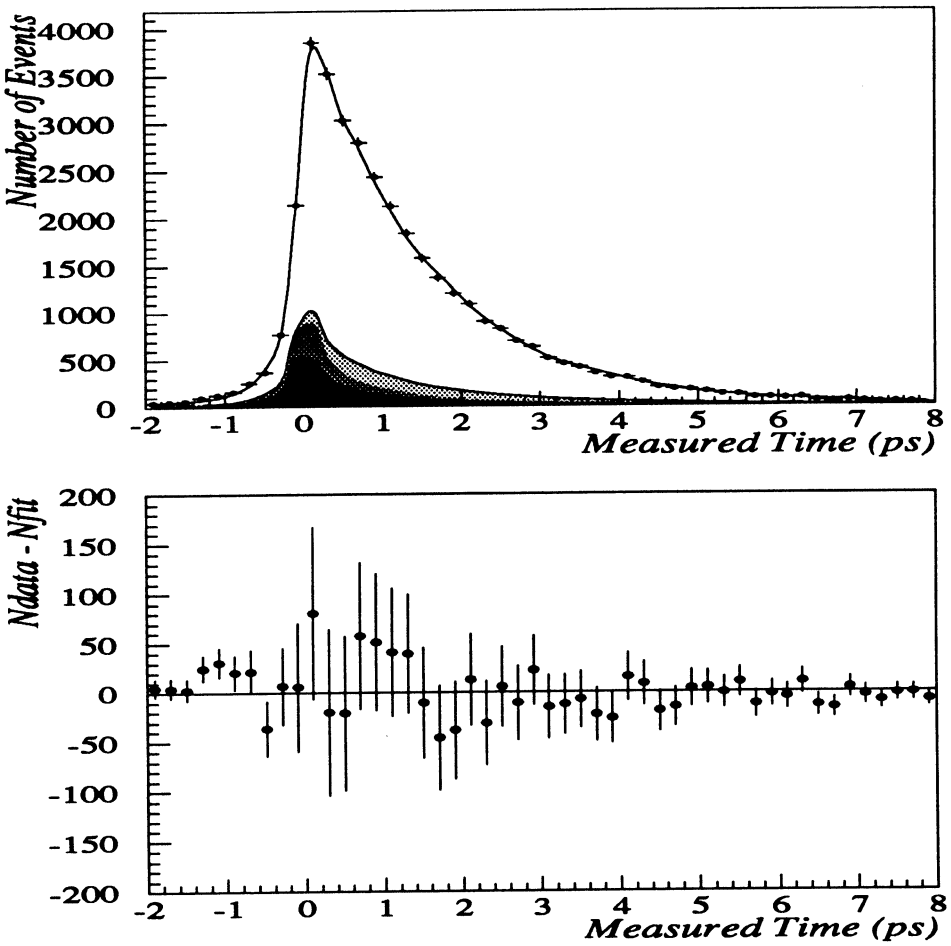

Figure 7: Measured time distribution in the Monte-Carlo. The points with error bars are the simulated data; the superimposed curve is the result of the fit. The time distributions corresponding to the different lepton sources are shown in various shades of gray: charm, background leptons, cascades, and (unshaded) primary b's, from bottom to top. The residuals (data-fit) are shown in the bottom half of the figure.

5 Δm_d Measurement

5.1 Resolution Effects and Background Subtraction

The measured lepton-signed jet charge for a pure sample of $b \rightarrow l$ decays, $Q^{prim}_{lH,msrd}(t_m)$, depends on:

- the true, time-dependent lepton signed jet charge $Q^{prim}_{lH,}(t)$; this is the quantity that contains the Δm_d , Δm_s information (Eq. 3);
- the true parent lifetime distribution, with lifetime τ_b ;

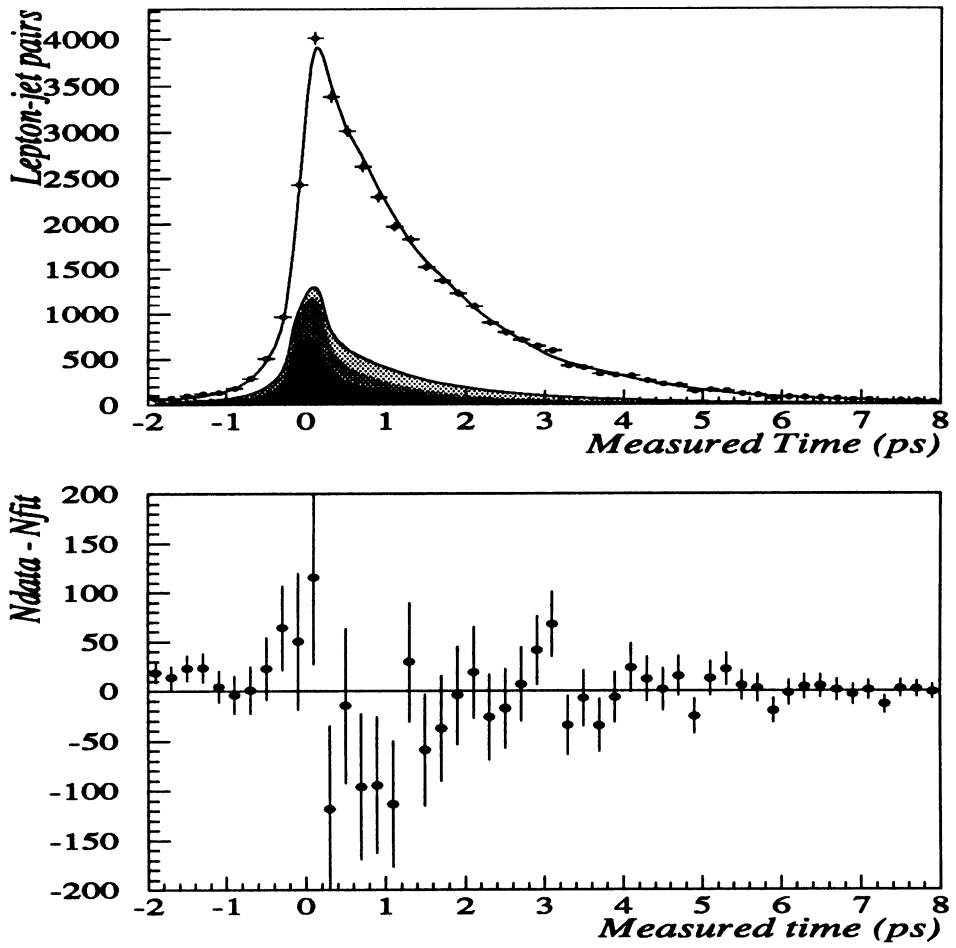

Figure 8: Measured time distribution in the 1991-93 ALEPH data. The points with error bars are the data; the superimposed curve is the result of the fit. The time distributions corresponding to the different lepton sources are shown in various shades of gray: charm, background leptons, cascades, and (unshaded) primary b's, from bottom to top. The residuals (data-fit) are shown in the bottom half of the figure.

- the vertexing efficiency for primary decays, $Eff^{prim}(t)$;
- the resolution in proper time for primary decays, $R_t^{prim}(t_m - t, t)$:

$$Q_{lH}^{prim}(t_m) = \frac{\int Q_{lH}(t) \times \frac{e^{-t/\tau_b}}{\tau_b} \times Eff^{prim}(t) \times R_t^{prim}(t_m - t, t) \times dt}{\int \frac{e^{-t/\tau_b}}{\tau_b} \times Eff^{prim}(t) \times R_t^{prim}(t_m - t, t) \times dt} \quad (5)$$

Similar considerations apply to the cascade contribution $Q_{lH,meas}^{casc}(t_m)$, which also carries mixing information. Account must also be taken of charm leptonic decays, which contribute the $Q^c(t_m)$ term, and of non-prompt leptons and misidentified hadrons, lumped in $Q^{bgd}(t_m)$. The value and time-dependence of the latter

is taken from the 1993 Monte-Carlo. The charm contribution is by definition time-independent, as it relies only on the hemisphere opposite to the lepton; the value of the mean charm charge is taken from the data [9].

Denoting by $Dtm(t_m)$ the normalized measured time distribution for each of the subprocesses of Table 1 in turn:

$$Dtm(t_m) = \frac{1}{N}\frac{dN}{dt_m}$$

the time-dependent fraction of each lepton source is given by

$$f_{source\ i}(t_m) = \frac{< f_{source_i} >_{time} \times Dtm^{source\ i}(t_m)}{\Sigma_{sources} < f_{source_j} >_{time} \times Dtm^{source\ j}(t_m)}$$

The measured lepton-signed jet charge for the whole data sample is the sum of the lepton-signed charges for each source, weighted by the time-dependent fraction each source contributes:

$$Q_{lH}^{msrd}(t_m) = \frac{f_{prim}Q_{lH}^{prim}Dtm^{prim} + f_{cas}Q_{lH}^{cas}Dtm^{cas} + f_cQ^cDtm^c + f_{bgd}Q^{bgd}Dtm^{bgd}}{f_{prim}Dtm^{prim} + f_{cas}Dtm^{cas} + f_cDtm^c + f_{bgd}Dtm^{bgd}} \quad (6)$$

where f_{prim}, f_{casc}, f_c and f_{bgd} are the time-averaged source fractions listed in Table 1.

5.2 Fitting Procedure

A two-parameter fit is performed to the time-dependence of $Q_{lH}^{msrd}(t_m)$, where the frequency of B_d^0 oscillations, Δm_d , and the average b jet charge Q_b are left free in the fit. Other parameters, including Δm_s , are kept fixed at the values listed in Table 2. Exclusive lifetimes are taken from Ref. [10]; the average b lifetime comes from Ref. [11]. The B_d and B_s fractions, and their errors (Sec. 6), were taken from Ref. [12] after correcting for differences in semileptonic branching ratios.

Table 2: Fixed parameters used in the Δm_d fit.

Parameter	Value
τ_{B_d} (ps)	1.614
τ_{B_s} (ps)	1.54
τ_b (ps)	1.537
τ_{B_d}/τ_b	1.05
f_d	0.401
f_s	0.114
Δm_s	Infinite
Q^c	0.0957
Q^{bgd}	0.0162
Flavor composition	See Table 1

There are two fundamental differences with the dilepton procedure:

- When both leptons in a dilepton event supply measured flight times, the event is treated as a whole: the distinction between charge at production time and at decay time is blurred, and a maximum likelihood fit is performed in two time dimensions. This is because what matters is the product of the two lepton charges, and this quantity is uniquely defined for each event. In contrast, in the present analysis, there is always one and only one time involved per lepton-jet pair, and so the fit is performed in one time dimension only. If two leptons are present in the event, each one of them is associated with its opposite-hemisphere jet; the two hemisphere charges are known to be correlated at the percent level only [3].

- The average b charge Q_b is left free in our fit, in order to avoid any Monte Carlo dependence related to jet charge modelling. In the dilepton analysis, the equivalent quantity would be equal to 1 in the absence of cascades, as the charge of a lepton is quantized. It turns out that because only a half-period of the oscillation is measurable before running out of statistics, the values of Δm_d and Q_b are correlated. This, in turn, implies that fitting additional parameters, such as the cascade fraction, as was done for the dileptons, may be impractical. Attempts to do so in our analysis indeed result in unstable fits. This is why we chose to fix the parameters listed in Table 2, and to account for the uncertainties affecting them in terms of systematic errors.

5.3 Results

The measured lepton-signed jet charge extracted from the 1991-93 ALEPH data, is shown in Fig. 9. A χ^2 fit [4] yields

$$\Delta m_d = 0.433^{+0.050}_{-0.032}\ ps^{-1} \quad ; \quad Q_b = 0.0779 \pm 0.0026 \tag{7}$$

where the errors are statistical only. The fit quality is satisfactory ($\chi^2/DOF = 46/48$). The results are consistent between electrons and muons (Table 3), as well as from one data year to the next (Table 4), albeit with a large upwards statistical fluctuation in 1992. Careful comparison of numerous control distributions, between 1992 and 1991+93, revealed no systematic problem.

We also verified that the measurement does not depend on the choice of the κ exponent that enters the definition of the jet charge. Repeating the analysis with κ=1.0 instead of 0.5, we find a value of Δm_d that is consistent, within 0.7 σ on the difference, with the result above.

As a consistency check, the same procedure was applied to the Monte Carlo (with the minor difference that Δm_s was set to the generated value, 1.85 ps^{-1}). The result is shown in Table 5. We verified, by dividing the data set in smaller subsamples and

[3] This reasoning neglects the fact that in dilepton events, the jet charge in one hemisphere is partially correlated with the charge of the lepton in that same hemisphere. Treating dilepton events as two independent lepton-jet pairs is therefore not rigorously correct. The impact on the magnitude of the error has not been investigated in detail; as it concerns only those dileptons with both times measured, i.e. about 5 % of our event sample, it is expected to be small.

[4] We verified the result is independent of the binning.

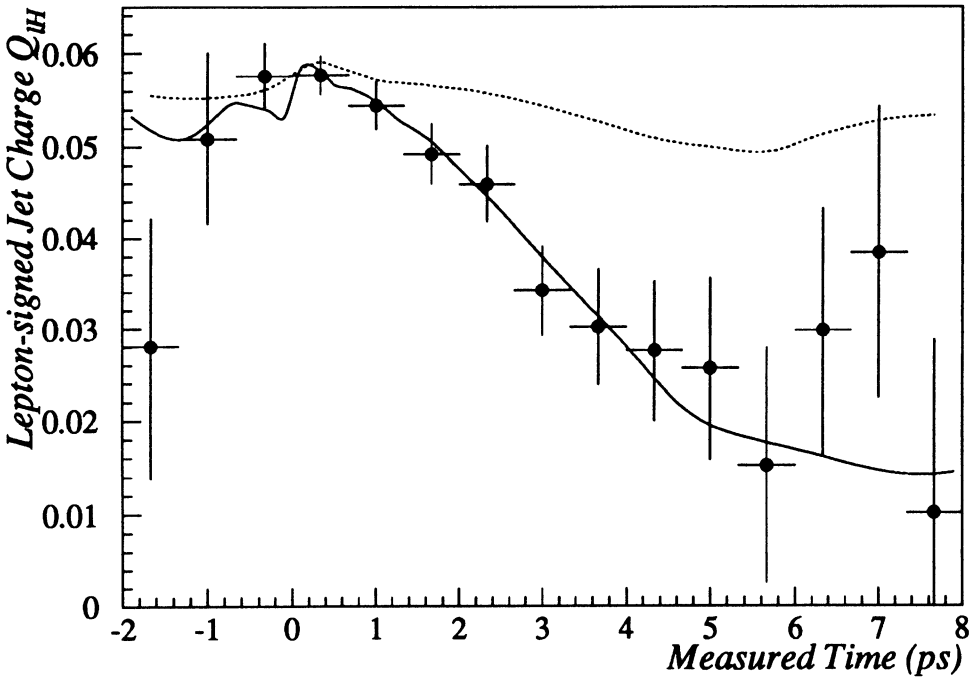

Figure 9: Lepton-signed jet charge vs. proper time. The points with error bars are the data ALEPH 1991-1993 data. The solid curve is the result of the fit; the dotted curve corresponds to the no-mixing hypothesis.

Table 3: Fitted Δm_d values for electrons and muons separately. Errors are statistical only.

Sample	Δm_d **(ps^{-1})**	**Lepton-jet pairs**
Electrons	$0.399 \pm^{0.071}_{0.064}$	14438
Muons	$0.458 \pm^{0.074}_{0.068}$	22069
All	$0.433 \pm^{0.050}_{0.032}$	36507

studying the distribution of the differences between generated and fitted values of Δm_d , that this difference is consistent with zero within 1.1 σ.

6 Systematic Errors

In order to estimate the systematic error, the above fitting procedure was repeated while varying, one at a time, the parameters left fixed in the fit. Table 6 summarizes the various contributions to the error.

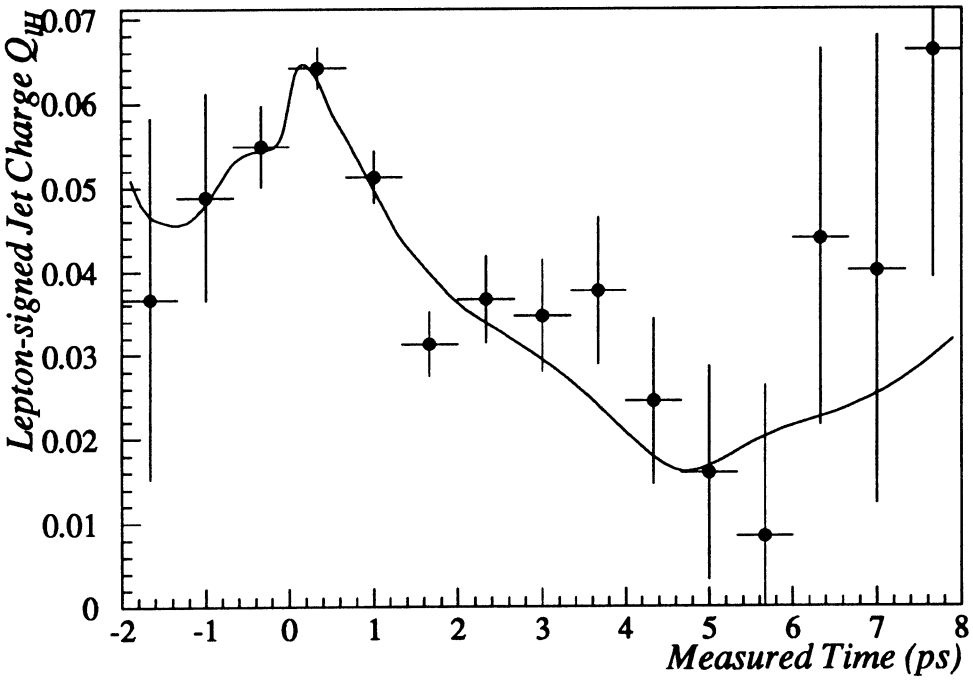

Figure 10: Lepton-signed jet charge vs. proper time. The points with error bars are the simulated Monte-Carlo data; the curve is the result of the fit.

Table 4: Fitted Δm_d values for the three data periods. Errors are statistical only.

Year	Δm_d (ps^{-1})	Lepton-jet pairs
1991	$0.364 \pm^{0.109}_{0.060}$	6094
1992	$0.618 \pm^{0.095}_{0.095}$	15854
1993	$0.350 \pm^{0.077}_{0.052}$	14559
91-92-93	$0.433 \pm^{0.050}_{0.032}$	36507

6.1 B_d and B_s lifetimes and fractions

The two largest systematic errors arise from the lifetime ratio τ_{B_d}/τ_b, and the B_d fraction f_d.

The latter effect naturally arises because the more B_d the sample contains, the stronger the time dependence of Q_{lH} is expected to be; as the latter is constrained by the data, Δm_d has to decrease to balance the assumed increase on f_d.

The dependence on the lifetime ratio is similar, but more subtle. An increase in τ_{B_d}, at fixed τ_b, implies a larger fraction of B_d at long proper times. As these "extra" B_d's happen to lie near the minimum of the cosine curve (half a period), their

Table 5: Comparison of fitted and generated Δm_d values for the Monte Carlo.

Quantity	Generated value	Fitted value
$\Delta m_d\ (ps^{-1})$	0.538	$0.627^{+.089}_{-.093}$
Q_b	.0790	$.0832 \pm .0039$

lepton-signed charge would "pull" down the average; as this is however constrained by the data, the fit compensates by reducing Δm_d .

Both of these effects occur because event statistics are exhausted by the time a half period has elapsed. If one could measure at least one full period, the frequency (Δm_d) and amplitude (Q_b) measurements would largely decouple, and the systematic sensitivity would be reduced.

A similar effect also explains the sensitivity to f_s: at very high Δm_s , the f_s term appears only in the amplitude. Increasing f_s shifts the predicted curve in Fig. 9 down; this is mostly absorbed by a change in the fitted amplitude, but some of the adjustment reflects itself onto Δm_d .

Finally, the B_s lifetime contributes to the error, because in the limit of infinite Δm_s , the average charge due to B_s-induced leptons is 0. When τ_{B_s} increases, the B_s population at large times increases, the mean charge decreases, and the effect is similar to that of τ_{B_d}.

6.2 Sample Composition

The next largest error is associated with the background fraction f_{bgd}, the large variation of which reflects our ignorance of the non-prompt lepton and misidentified hadron background. Because the average background charge (resp. mistag rate) is considerably smaller (resp. larger) than that in $b \to l$ events, an increase in f_{bgd} reduces the expected amplitude at short times; the fit attempts again to compensate.

Other fractions influencing the sample composition (f^{prim}, f^{cas}, f^{c}) are varied by amounts suggested by the results of Ref. [7].

6.3 Resolution Functions

The error associated with the time resolution is estimated by fitting Δm_d with and without the resolution-widening correction discussed in Sec. 4.3.

As was pointed out in Sec. 4.3.3, there remains a systematic disagreement between the measured time distribution in data compared to Monte-Carlo. To ascertain the potential impact on Δm_d , the measurement was repeated by increasing the minimum proper time considered in the fit, progressively excluding the region of poor agreement (Fig. 8). The result, shown in Fig. 11, shows our result is stable within statistics.

The error labelled "Energy correction" was evaluated by reweighting the events so that the boost distribution in the data and in the Monte Carlo become identical.

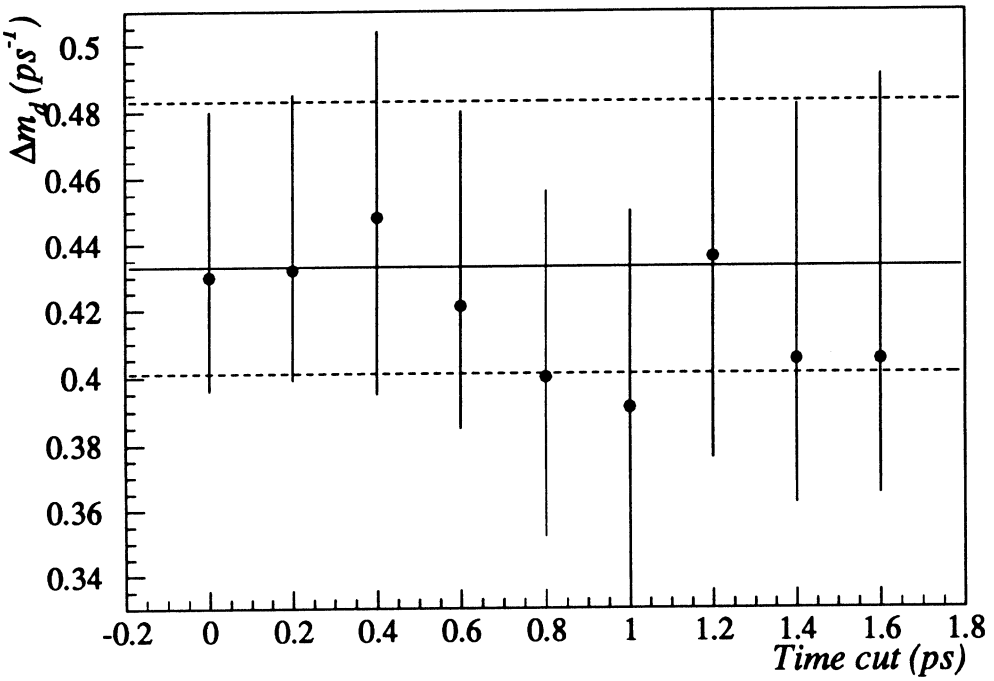

Figure 11: Fitted value of Δm_d , as a function of the minimum measured time considered in the fit. The error bars are the full statistical error on each measurement, and are therefore highly correlated.

The associated systematic error is very small.

6.4 Other Errors

The relative fractions of cascades, in B_d and B_s decays, are different from each other in the Monte Carlo because of different decay channels and branching ratios. The latter are however poorly known. The error quoted corresponds to setting them arbitrarily equal to each other.

The average jet charges of charm- and background-associated leptons are varied within, respectively, the published error [9], and the statistical error in the MC (which corresponds to a $\pm 50\%$ relative variation).

Finally, the error associated with Δm_s is evaluated by refitting Δm_d with $\Delta m_s = 6$.

7 Conclusions

Using an inclusive sample of lepton-jet events, we have measured, in the 1991-1993 ALEPH data,

$$\Delta m_d = 0.433\ ^{+0.050}_{-0.032}\,(stat.)\ ^{+0.062}_{-0.064}\,(syst.)\ ps^{-1} \tag{8}$$

The systematic error is dominated by the uncertainty on the τ_{B_d}/τ_b lifetime ratio, and by the fraction of B_d in the sample.

By comparison, the corresponding ALEPH dilepton result is [2]

$$\Delta m_d = 0.45\ \pm 0.05\,(stat.)\ ^{+0.09}_{-0.08}\,(syst.)\ ps^{-1} \tag{9}$$

Care should be taken in combining these two numbers, as the dilepton sample is largely included in our lepton-jet sample, and the systematic errors are partially correlated.

References

[1] D. Buskulic *et al.* (ALEPH Collab.), An Investigation of B_d^0 and B_s^0 Oscillation, Phys. Lett. **B 322** (1994) 441-458.

[2] R. Forty, Measurement of the B_d^0 Oscillation Frequency and a lower limit for the B_s^0, ALEPH 94-077, PHYSIC 94-066 (1994).

[3] D. Buskulic *et al.* (ALEPH Collab.), Limit on B_s^0 Oscillation using a Jet Charge Method, in preparation.

[4] D. Buskulic *et al.* (ALEPH Collab.), Measurement of $B - \overline{B}$ mixing at the Z using a jet-charge method, Phys. Lett. **B 284** (1992) 177-190.

[5] S. Emery, presentation to the ALEPH Mixing and Lifetime meeting, 26 November 1994.

[6] D. Abbaneo *et al.*, Lepton and Jet Definitions for the Lepton Paper, ALEPH 92-101, PHYSIC 92-90 (1992).

[7] D. Buskulic *et al.* (ALEPH Collab.), CERN-PPE/94-017 (1994), submitted to Z. Phys; D. Buskulic *et al.* (ALEPH Collab.), CERN-PPE/94-023 (1994), submitted to Nucl. Instr. and Meth.

[8] E. Martin, Measurement of heavy flavours lepton's b purity, ALEPH 94-157, PHYSIC 94-134 (1994).

[9] P. Perrodo, On Charm Charge Separation, ALEPH 94-066 PHYSICS 94-058.

[10] P. Roudeau, Heavy Flavours (effects from strong interactions), invited talk at the X^{th} Rochester conference on High Energy Physics, Glasgow (1994).

[11] Review of Particle Properties, Phys. Rev. **D 50** 3 (1994) 1173.

[12] O. Hayes, Estimate of b-Hadron Fractions in $Z \rightarrow b\bar{b}$ Events, ALEPH 94-197, PHYSIC 94-167 (1994).

Source of systematic uncertainty	Δm_d variation (ps^{-1})
$\frac{\tau_{B_d}}{\tau_b} \pm 0.06$	-0.040 $+0.040$
$\tau_{B_s} \pm 0.15\ ps$	-0.019 $+0.020$
$\tau_b \pm 0.037\ ps$	$+0.005$ -0.005
$f_d \pm 0.028$	-0.025 $+0.031$
$f_s \pm 0.035$	-0.014 $+0.014$
$f_{d,s}^{cas} = f_{d,s}^{prim}$	-0.016
$f^{prim} \pm 4.5\ \%$	$+0.001$ -0.001
$f^{cas} \pm 15\ \%$	-0.010 $+0.010$
$f^{c} \pm 10\ \%$	-0.001 $+0.001$
$f^{bgd} \pm 40\ \%$	$+0.020$ -0.022
$Q^{c} \pm 0.012$	-0.008 $+0.008$
$Q^{bgd} \pm 0.008$	-0.006 $+0.006$
Time resolution	-0.018
Energy correction	-0.002
$\Delta m_s = 6\ ps^{-1}$	-0.003
Quadratic sum :	$+0.062$ -0.064

Table 6: Contributions to the systematic error on Δm_d . The numbers in the left column indicate the range over which each parameter is varied.